

The M - σ relation from the disruption of binaries from the galactic bulge

Erez Michaely^{*} and Douglas Hamilton

Astronomy Department, University of Maryland, College Park, MD 20742

Accepted XXX. Received YYY; in original form ZZZ

ABSTRACT

We present a novel explanation of the well known $M_{\bullet} - \sigma$ relation. In a triaxial potential binaries with chaotic orbits within a sphere that encompass ~ 100 times the mass of the super-massive black-hole (SMBH) have a finite probability to be tidally disrupted by the SMBH. As a result one component loses energy and might itself break apart tidally and accreted onto the SMBH. More significantly, the other component, which gains energy, returns to the bulge and equilibrates its excess energy with the environment thereby changing the kinetic temperature, hence the velocity dispersion. We develop a mathematical model and find that its results are in agreement with the observed relation.

1 INTRODUCTION

The mass of a super massive black-hole (SMBH), M_{\bullet} , is correlated with several properties of its host galaxy. M_{\bullet} has correlations with the stellar luminosity (Gültekin et al. 2009), $M_{\bullet} - L_{*}$ relation; with stellar mass, specifically the mass of the bulge (for disk galaxies) or the mass of the galaxy itself (for elliptical galaxies) (McConnell & Ma 2013). Surprisingly, the tightest relation is with the stellar velocity dispersion of the spheroid surrounding the SMBH, the well known $M_{\bullet} - \sigma$ relation (Ferrarese & Merritt 2000; Zubovas & King 2019; Gültekin et al. 2009). These relations provide important evidence for the co-evolution of both the SMBH and the host galaxy which have interesting ramifications in many fields of astrophysics. In this work we focus on the $M_{\bullet} - \sigma$ relation, namely, $\log M_{\bullet} = \gamma + \beta \log \sigma$.

The first $M_{\bullet} - \sigma$ relation observational papers were published almost 20 years ago (Ferrarese & Merritt 2000; Gebhardt et al. 2000). Both teams reported their results with almost no scatter, but with different slopes. Ferrarese & Merritt (2000) reported $\beta = 4.80 \pm 0.50$ while Gebhardt et al. (2000) found $\beta = 3.75 \pm 0.30$. In course of time the $M_{\bullet} - \sigma$ relation was measured for more galaxies. van den Bosch (2016) calculated $\beta = 5.35 \pm 0.23$ and $\gamma = -4.0 \pm 0.5$; while McConnell & Ma (2013) got $\beta = 5.64 \pm 0.32$ and $\gamma = 8.21 \pm 0.05$. Regardless of the precise value, the $M_{\bullet} - \sigma$ relation is both remarkable and surprising. The SMBH dominates gravitationally the immediate vicinity of its location, the sphere of influence, which has typically radius of a few parsecs. However, the radius of the spheroids surrounding the SMBH have typical radii of a kilo parsec (or more), so the SMBH cannot govern the dynamics of it. Yet the $M_{\bullet} - \sigma$ relation is observed in the local Universe, at redshifts $z \lesssim 0.1$, corresponding to time later than $t \sim 12$ Gyr after the Big Bang.

Shen et al. (2015) used data from the Sloan Digital Sky Survey in order to search for the $M_{\bullet} - \sigma$ relation as a function

of redshift. They report that no evidence of such evolution and the $M_{\bullet} - \sigma$ relation holds up to $z \approx 1$, where the age of the Universe at $z \approx 1$ is ~ 6 Gyr. This suggests that the process that leads to the $M_{\bullet} - \sigma$ relation should saturate by $t \sim 6$ Gyr.

Generally speaking the proposed explanations for the $M_{\bullet} - \sigma$ relation could be grouped into three categories (Zubovas & King 2019). First, “central limit-like theorem”, (e.g. Peng 2007; Jahnke & Macciò 2011). In these sets of explanations, the underlining assumption is that the $M_{\bullet} - \sigma$ relation emerges not due to co-evolution of the central BH and the host galaxy, but due to hierarchical assembly of BH and stellar mass through galaxy mergers. The mergers from an initially uncorrelated distribution of BH and stellar masses in the early universe produce the observed correlations. Second, “Gas feed rate” (e.g. Haan et al. 2009; Anglés-Alcázar et al. 2013, 2015). This theory proposes that the SMBH mass growth is due to the feeding of gas which in turn is a function of the host galaxy characteristics, specifically galaxy-scale torques on the gas that govern the inflow of gas to the SMBH and hence govern the mass of the SMBH. Third, and arguably the most accepted explanation is the “Feedback mechanism”. This process relies on the energy released from the accretion of mass on to the SMBH. The energy released may affect the entire galaxy which can regulate, in turn, the mass infall to the SMBH. Feedback can come in several forms, changing the star formation rate or regulating the infall mass rate itself onto the SMBH.

Almost 20 years ago Merrit and Poon published a series of four papers on triaxial nuclear bulges containing an SMBH (Poon & Merritt 2001, 2002, 2004; Merritt & Poon 2004, hereafter PM1;PM2;PM3;MP4). In PM1 they investigated the orbital motion of test particles in a triaxial nucleus hosting an SMBH. The stellar density profile they consider follows a power law $\rho_{*} \propto r^{-\gamma}$ with $\gamma = \{1, 2\}$. For triaxial potentials with a central point mass the phase space is

naturally divided into three regions defined by the distance (energy) from the center. The innermost region, within the sphere of influence of the SMBH, with radius $r_h \approx GM_\bullet/\sigma^2$, hosts low energy orbits, e.g. tubes, pyramids and bananas, and the trajectories are mainly regular and avoid close passages with the center of the potential. However, at higher energies the pyramid orbits become increasingly chaotic. The transition to the chaotic regime occurs rapidly, i.e. sharply in space. Beyond the sphere of influence is the second region with intermediate radii, the scattering zone region. In this region, the SMBH acts as a scattering center for almost all the center-filling trajectories. The second region is located from the edge of the sphere of influence outward until the radius that encompass a total mass of $\sim 50 - 100M_\bullet$. In this region the orbits are a mix of “regular” orbits which avoid the center of potential and “chaotic” orbits which pass near the center of potential one per crossing time. The fraction of chaotic orbits is $f_c \approx 0.5$ (MP4). The third region, the outermost region, hosts the highest orbital energies, and the rest of the mass of the spheroid. The phase space is a complex mixture of chaotic and regular trajectories. This region has a mixture of chaotic and regular orbits.

In PM2 they showed that the triaxial potential is retained in time. Hence one cannot overlook the importance of stellar dynamics in the environments of triaxial galactic potentials. PM3 investigated the fraction of chaotic orbits for 3 triaxial shapes: almost prolate, almost oblate and maximally triaxial. They found that $\sim 50\%$ of the mass is assigned to chaotic orbits. The last paper of the series, MP4, present a mathematical model of the galactic center and calculates the rate of single-star disruption from chaotic orbits in order to explain the $M_\bullet - \sigma$ relation.

In this paper we build on the work of MP4 and expand their modeling to binaries that are tidally disrupted by the SMBH. In what follows, we describe the co-evolution of the SMBH mass growth together with the change in the kinetic temperature of the spheroid due to disruption of binaries from the bulge. As a result of the binary disruption, a fraction of single stars will experience a stellar tidal disruption event (TDE), while the surviving star re-equilibrates its excess with the bulge altering its kinetic temperature and hence the velocity dispersion.

In section 2 we describe the model both qualitatively and quantitatively. In section 3 we present the results of the numerical simulation while in section 4 we discuss implications and caveats and summarize the manuscript.

2 THE MODEL

2.1 Qualitative description

In this subsection we briefly describe the dynamical model and assumptions in a qualitative manner. We assume triaxial potentials for all bulges with isotropic mass distributions. The number of systems (either binaries or single stars) is $N = N_b + N_s$ where $N_{b(s)}$ is the number of binaries (singles). Furthermore, we assume that the initial binary fractions equal to f_{binary} , i.e. the mass in binaries is $f_{\text{binary}} \times M_{\text{bulge}}$. For simplicity we set all binaries components to have the same mass $m_1 = m_2 = 1M_\odot$ in circular orbits. The semi-major axis (sma) is distributed from some

distribution function f_a . PM1-3 and MP4 showed that the centrophilic orbits are about half of the stellar mass of the second spatial region, hereafter bulge mass, i.e. half of the binaries. In our model we calculate the rate that binaries enter the binary tidal disruption radius, r_{bu} . As a result, from this binary disruption one component returns to the bulge with typically more specific energy, hence the energy budget of the bulge changes and so the velocity dispersion evolves. The other component, which is typically captured/disrupted by the SMBH, may change the mass of the SMBH. Additionally, we account for the binary ionization process in the bulge, due to random interaction with passing stars.

We model the binary tidal disruption with the impulse approximation. The impulse approximation holds when the binary may be considered stationary while interacting with the SMBH. The two relevant timescales are the binary orbital period, P and the interaction timescale, $t_{\text{int}} \equiv q/v_q$ where q is the closest approach of the binary center of mass to the SMBH and v_q is the center of mass velocity at q (Agnor & Hamilton 2006).

In order to verify the validity of the impulse approximation for a binary interaction with the SMBH, we perform a set of 1000 numerical simulations. Using an N-body integrator (Hut 1981) we simulate a circular binary with two component masses of $m_1 = m_2 = 1M_\odot$, with a center of mass on a hyperbolic trajectory around an SMBH with mass of $M_\bullet = 4 \times 10^6 M_\odot$. We initiate all binary center of mass velocities to be equal to the bulge velocity dispersion, namely $\sigma = 200\text{kms}^{-1}$. Next we set the binary semi-major axis (sma), a , the pericenter distance, to the SMBH, q , and the binary mean anomaly, m . We sample 10 equally spaced sma values in log space between 10^{-2}AU and 10^2AU . Additionally, we set 10 equally spaced pericenter values in log space between r_* and r_{bu} , where r_* is the tidal disruption radius of a single star, given by (1) and r_{bu} is the binary tidal disruption radius, given by (2); where m_* and R_* is the mass and radius of a star and $m_b = m_1 + m_2$ is the total mass of the binary system.

$$r_* = \left(\frac{3M_\bullet}{m_*} \right)^{1/3} R_* \quad (1)$$

$$r_{\text{bu}} = \left(\frac{3M_\bullet}{m_b} \right)^{1/3} a \quad (2)$$

Furthermore, we set 10 equally spaced mean anomaly values, m between 0 and π . We align the binary angular momentum vector with the angular momentum of the hyperbolic trajectory, i.e. setting the inclination to zero, for simplicity.

For each simulation that underwent binary disruption, we record the outcomes of the components, namely one component is always ejected and the other is either ejected or captured/disrupted. We emphasize that the initial trajectory is hyperbolic hence both components may escape after the fly-by. Next we focus on the component with the higher kinetic energy, we calculate its velocity at the edge of the Hill sphere, r_h . Using conservation of energy where v_{bu} is the circular velocity around the binary center of mass:

$$v_b = \left(2GM_\bullet \left(\frac{1}{r_h} - \frac{1}{r_{\text{bu}}} \right) + v_{\text{bu}}^2 \right)^{1/2}. \quad (3)$$

Figure 1 presents the velocity of the escaper at the edge of the Hill sphere as a function of initial binary sma.

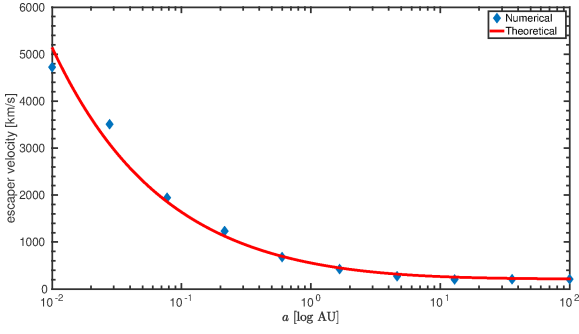


Figure 1. Verification of the impulse approximation treatment. The value of the escaper’s velocity at the edge of the radius of influence as a function of binary sma. The blue diamonds are the calculated velocity of the escaper at the edge of the sphere of influence, from the N-body simulation. The red solid line is the predicted values of the velocity from the theoretical treatment of the impulse approximation. The agreement is good.

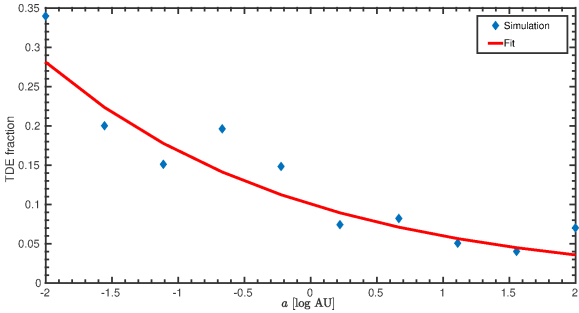


Figure 2. Blue diamonds are the fraction of TDE as a function of binary sma from the numerical simulation. Red solid line is the best fit $f_{\text{TDE}} = 0.1 \times \left(\frac{a}{\text{AU}}\right)^{-0.2244}$ for $M_{\bullet} = 1 \times 10^6 M_{\odot}$ and $\sigma = 200 \text{ km s}^{-1}$.

Next we focus on the component with the lower kinetic energy.

The less energetic component

In the previous subsection we focused on the more energetic component, and approximated its velocity when reaching the bulge boundary, i.e. the edge of the sphere of influence. In this subsection we focus on the less energetic component. This component acquires a new Keplerian trajectory upon binary disruption. We record its closest approach to the SMBH and compare it to r_* , the tidal disruption radius of a single star. If the closest approach is smaller than r_* than we flag it as a tidal disruption event (TDE). Figure 2 shows the fraction of single-star TDE out of the disrupted binary sample as a function of binary sma from the simulation. We found the best fit for the TDE fraction as a function of binary sma, a , to be the following:

$$f_{\text{TDE}}(a) = 0.1 \times \left(\frac{a}{\text{AU}}\right)^{-0.2244}. \quad (4)$$

2.2 Quantitative description

Mathematical framework

In this subsection we describe in detail the mathematical model accounting for the physical processes.

There are three relevant length scales in the problem regarding the binary break-up and the tidal disruption of one of the stars from the binary. First, r_{bu} , is the binary tidal disruption radius from the SMBH for a binary with sma a and total binary mass m_b , as defined in equation (2). For an SMBH mass of $M_{\bullet} = 10^6 M_{\odot}$ and a binary with sma of $a = 1 \text{ AU}$ and total mass of $m_b = 2 M_{\odot}$, the value of binary tidal disruption radius is of the order of $r_{\text{bu}} \approx 100 \text{ AU}$. Second, q , is the pericenter distance of the binary trajectory from the SMBH. Third, r_* , is the single star tidal disruption radius for a star with radius R_* and mass m_* defined in equation (1). For a sun like star the value of the tidal disruption radius is approximately $r_* \approx 1 \text{ AU}$.

The bulge is naturally divided into three spatial regions for a triaxial potential with a central point mass (the SMBH) as mentioned in section 1. In this work we focus on the second region, the scattering zone, where roughly half of the mass are in chaotic trajectories. The total stellar mass in it is $\sim 100 M_{\bullet}$.

We use the model and notations for the galactic nucleus described in MP4. The stellar density is given by

$$\rho_* = \rho_0 m^{-\gamma} \quad (5)$$

we get set $\rho_0 = 1$ because of the scale free nature of the density profile with no loss of generality, m is defined by the following equation of an ellipsoid:

$$m^2 = \frac{x^2}{a^2} + \frac{y^2}{b^2} + \frac{z^2}{c^2}. \quad (6)$$

The triaxial parameter T is given by

$$T \equiv \frac{a^2 - b^2}{a^2 - c^2} \quad (7)$$

where $T = 0.5$ is maximally triaxial.

We focus on the case where $\gamma = 2$, the isothermal sphere with particle mass of m_b . In this steep cusp profile the potential is given by equation 7 in PM1. It is convenient to use the corresponding circular orbit energy in the analogous spherical model is

$$E_c(r) = 4\pi\delta^2 \left[\ln\left(\frac{r}{\delta}\right) - 1 \right] \quad (8)$$

where $\delta = (abc)^{1/3} = 0.734$ for $T = 0.5$. This function is given in model units specified in MP4. In this system the units of mass, length and time is given by the following:

$$[M] = M_{\bullet} \quad [L] = (2\pi\delta^2) r_h \quad [T] = (2\pi\delta^2)^{3/2} \sqrt{\frac{r_h^3}{GM_{\bullet}}}. \quad (9)$$

Here we follow MP4 to define $r_h = GM_{\bullet}/\sigma^2$ as the radius in the spherical model containing a stellar mass of $2M_{\bullet}$.

Given equations (5) and (8) we write the total mass of stars per specific energy in real units:

$$\mathcal{M}(E) = \frac{2\sqrt{6}}{9} \frac{M_{\bullet}}{\sigma^2} \exp\left(\frac{E - E_h}{2\sigma^2}\right) \quad (10)$$

where $E_h \equiv E(r_h)$. We define $\mathcal{M}_b(E) \equiv (N_b/N) \mathcal{M}(E)$ to be the total mass in binaries with specific energy shell E . The corresponding density as a function of distance in model units and real units is:

$$\rho_* = \rho_h \left(\frac{r}{r_h} \right)^{-2} = \frac{M_\bullet}{2\pi r_h} r^{-2}. \quad (11)$$

where we have chosen $\gamma = 2$ in equation 5 with the normalization $\rho_h = M_\bullet / (2\pi r_h^3)$ which is the stellar density at the edge of the sphere of influence.

MP4 present their results on the number of encounters per unit time for a chaotic orbit, with some energy E , within a distance d from the center of the potential, i.e. the SMBH. They found a linear scaling with d combined with the gravitational focusing from the SMBH, where the cross section scales linearly with d as well, the number of encounters within a distance d per unit time scales like $N_{<d} \propto d^2$ for a given energy shell. Generally they found the rate per unit time per unit distance is

$$A(E) \approx 1.2 \left(\frac{\sigma^5}{(GM_\bullet)^2} \right) \exp\left(\frac{-(E - E_h)}{\sigma^2} \right). \quad (12)$$

Binary disruption calculation

The rate at which a binary on a chaotic orbit of specific energy E experiences closest approach to the SMBH within a distance d is given by $A(E) \times d$. Together with equation (10) we can write the rate of binary disruption as a function of time, t , sma, a and energy, E , by setting $d = r_{bu}$

$$\Gamma_1(a, E, t) = f_a(a) A(E) r_{bu}(a) \frac{f_c M(E)}{m_b} \exp(-A(E) r_{bu}(a) t). \quad (13)$$

We remind that $f_c M(E) / m_b$ is the number of binaries in chaotic orbits and $f_a(a)$ is the sma distribution. This equation does not account for binary ionization in the bulge due to random interaction with passing systems. These interactions may disrupt binaries resulting in a reduction of the number of available binaries to be disrupted by the SMBH. In order to account for this we calculate the half-life time of a binary with sma a and total mass m_b in an environment with stellar density ρ_* and velocity dispersion σ by (Bahcall et al. 1985)

$$t_{1/2}(a, E) = 0.00233 \frac{\sigma}{G\rho_*(E)a}. \quad (14)$$

As a result the corrected binary disruption rate is

$$\Gamma(a, E, t) = \Gamma_1(a, E, t) \exp(-t \ln 2 / t_{1/2}(a, E)). \quad (15)$$

Implications from binary disruption

Once a binary, in a hyperbolic trajectory, enters r_{bu} it is disrupted into its two components stars. One star receives energy and return to the bulge, m_1 , while the other star with mass m_2 may be capture or disrupted by the SMBH. As a result the mass of the bulge is reduced by m_2 , while the mass of the SMBH increases by the amount of the accreted mass from a possible single star TDE, Δm_{acc} . We define $\Delta m_{acc} \equiv m_2 \times f_{TDE}(a) \times f_{acc}$ where f_{TDE} is the fraction of TDE from the set of binary tidal disruptions, and $f_{acc} = 1/2$ (PM3) for $M_\bullet < 10^8 M_\odot$ and $f_{acc} = 1$ for $M_\bullet > 10^8 M_\odot$.

Additionally, once m_1 returns back to the bulge it arrives with speed $v_1(a)$. The bulge is modeled as an isothermal sphere with Maxwellian distribution of velocities. In this case a kinetic temperature of the bulge can be defined as a function of the velocity dispersion:

$$k_B T_{bulge} = \bar{m} \sigma^2 = \frac{\bar{m} \bar{v}^2}{3} \quad (16)$$

where \bar{m} is the average mass of the components in the bulge, \bar{v}^2 is the mean square speed of the components and T_{bulge} is the kinetic temperature of the bulge. Therefore, one can determine the equivalent kinetic temperature of a single star to be

$$T_2 = \frac{m_1 v_1^2(a)}{k_B}. \quad (17)$$

In this work we assume m_1 equilibrates its energy with the environment of the bulge, we address this assumption in section 4. The change in bulge temperature per unit time, due to this process is

$$\frac{dT_{bu}}{dt} = \left(\frac{1}{N} \right) \int_{a_{min}}^{a_{max}} da \int_{E_h}^{E_{edge}} dE \times \Gamma(a, E) \times (T_2(a) - T_{bulge}). \quad (18)$$

Where E_{edge} is the energy at the end of the second spatial region and a_{min} , a_{max} are the boundaries of the sma. Moreover, binaries in the bulge get disrupted continuously due to random interaction with passing stars. These process changes both the number of components (from a binary to two single stars) and the specific energy of the bulge. The two stars come with kinetic temperature of

$$T_3(a) = \frac{2m_*}{k_B} \left(\frac{1}{2} \sqrt{\frac{Gm_b}{a}} \right)^2. \quad (19)$$

The rate where $N_b(t)$ decreases both due to the ionization process and the binary disruption from the SMBH is given by the following:

$$\frac{dN_b(t)}{dt} = - \int_{a_{min}}^{a_{max}} da \int_{E_h}^{E_{edge}} dE \times \left(\frac{\mathcal{M}_b(E)}{m_b} f_a(a) \frac{\ln 2}{t_{1/2}(a, E)} + \Gamma(a, E, t) \right). \quad (20)$$

We calculate the change in temperature due to this process by

$$\frac{dT_{ion}}{dt} = \int_{a_{min}}^{a_{max}} da \int_{E_h}^{E_{edge}} dE \frac{1}{N} \frac{dN_b(t)}{dt} (T_3(a) - T_{bulge}), \quad (21)$$

which together with

$$\sigma(t) = \left(\frac{k_B T(t)}{\frac{1}{N} (N_b(t) \times m_b + N_s(t) \times m_*)} \right)^{1/2} \quad (22)$$

allows us to calculate the evolution of the velocity dispersion.

Mass accretion to the SMBH

The mass accretion to the SMBH originates from TDEs after binaries are disrupted whence their pericenter distances are closer than r_{bu} . Some fraction from all disrupted binaries ends up with a single star TDE, $f_{\text{TDE}}(a)$. In this work we assume that half of the mass of the disrupted star is accreted (Stone et al. 2019) for $M_{\bullet} < 10^8 M_{\odot}$ and all of the mass of the disrupted star is accreted for $M_{\bullet} > 10^8 M_{\odot}$.

$$\frac{dM_{\bullet}(a, E)}{dt} = f_{\text{TDE}}(a) \times \Gamma(a, E) \times m_{*}. \quad (23)$$

3 RESULTS

In this section we present results for a wide range of plausible initial conditions and binaries properties in order to show the robustness of the proposed process. In subsection 3.1 we show a representative example of the time evolution of some model parameters. In subsection 3.2 we describe the initial conditions used and present the evolution of the $M_{\bullet} - \sigma$ relation for the considered calculation.

3.1 Time evolution: Representative example

For the representative example we consider an SMBH with initial mass of $M_{\bullet} = 10^7 M_{\odot}$ embedded in a bulge with $M_{\text{bulge}} = 5 \times 10^8 M_{\odot}$. We emphasize that the definition of M_{bulge} is chosen to be the total mass of the second spatial region and not the total mass of the spheroid surrounding the SMBH. The binary fraction is unity, i.e. all the bulge mass is in binaries. The total mass of each binary is $2M_{\odot}$ with equal mass components in a circular orbit. The distribution of sma of the binaries is log uniform with $a \in \{a_{\text{min}}, a_{\text{max}}\}$ with $a_{\text{min}} = 0.01 \text{AU}$ and $a_{\text{max}} = 100 \text{AU}$. The initial velocity dispersion is $\sigma_0 = 67.5 \text{kms}^{-1}$ and the fraction of TDE as a function of sma is taken from (4). The initial value of the velocity dispersion is smaller than the predicted value from the $M_{\bullet} - \sigma$ relation, almost by a factor of two. Figure (3) present the time evolution of the velocity dispersion and the mass of the SMBH. The SMBH accretes small amount of mass, roughly 1% of its initial mass. However the velocity dispersion is changing significantly by almost a factor of two. The final value of σ agrees well with the observed $M_{\bullet} - \sigma$ relation. This simulation shows promise and so we undertake a thorough exploration of parameter space.

3.2 Main results

We consider two binary sma distributions: log-uniform and log-normal (Duchêne & Kraus 2013). For the log-uniform case we assume the binary sma are distributed from $a \in [a_{\text{min}}, a_{\text{max}}]$, and $a_{\text{min}} = 0.01$ and $a_{\text{max}} = 100 \text{AU}$ where the lower bound corresponds to contact binaries for a binary with two $1M_{\odot}$ components. Furthermore, we assume that the mass of the surrounding spheroid is $M_{\text{bulge}} = \alpha \times M_{\bullet,0}$ where $M_{\bullet,0}$ is the initial mass of the SMBH, and $\alpha = 50$. The 10 initial values of the SMBH masses and 10 values of the velocity dispersion are chosen to be evenly distributed in $\log M_{\bullet}$ and $\log \sigma$. The mass boundaries are $M_{\bullet, \text{min}} = 10^5 M_{\odot}$ and $M_{\bullet, \text{max}} = 10^8 M_{\odot}$ while the velocity dispersion boundaries are $\sigma_{0 \text{min}} = 30 \text{kms}^{-1}$ and $\sigma_{0 \text{max}} = 120 \text{kms}^{-1}$.

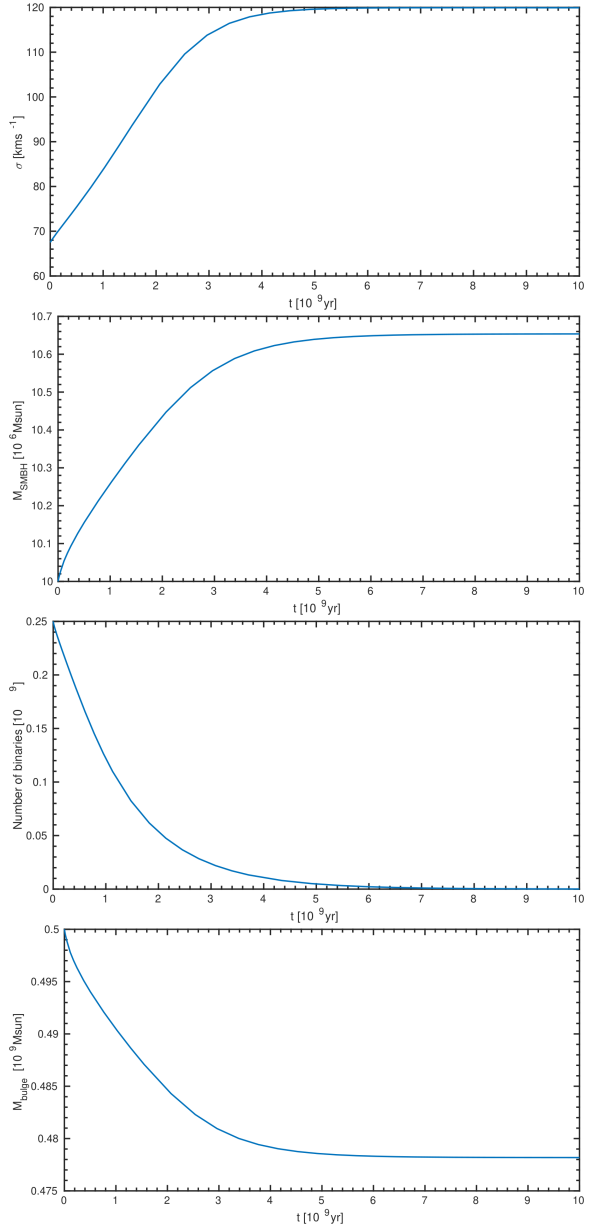


Figure 3. The time evolution the velocity dispersion and the SMBH mass. For $\alpha \equiv M_{\text{bulge}}/M_{\bullet} = 50$, $M_{\bullet} = 1 \times 10^7 M_{\odot}$, $\sigma_0 = 67.5 \text{kms}^{-1}$, $a_{\text{min}} = 0.01 \text{AU}$, $a_{\text{max}} = 100 \text{AU}$, log uniform, $f_{\text{TDE}} = 0.1 \times \left(\frac{a}{\text{AU}}\right)^{-0.2244}$. The binary fraction used here was $f_{\text{binary}} = 1$. The upper plot presents the evolution of the velocity dispersion σ in time. The second from the top presents the change in the SMBH mass as a function of time. The third from the top shows the decrease in the numbers of binaries in the bulge due to both ionization and binary disruption by the SMBH (20). The bottom panel presents the change in the mass of the bulge.

Figure 4 presents the results of 100 integrations with $t_{\text{final}} = 1.2 \times 10^{10} \text{yr}$ that corresponds to $z = 0.1$. It is clear that almost all initial condition within the mass range of $5 < \log M_{\bullet} < 7$ evolve into the region were the $M_{\bullet} - \sigma$ is observed. However, the upper range of masses, $\log M_{\bullet} > 7$ evolve into the observed region only for sufficiently high initial velocity dispersion, i.e. $\sigma_0 \gtrsim 80 \text{kms}^{-1}$. In order to demonstrate that the convergence does occur for the larger masses but on only on unphysical timescale we present in

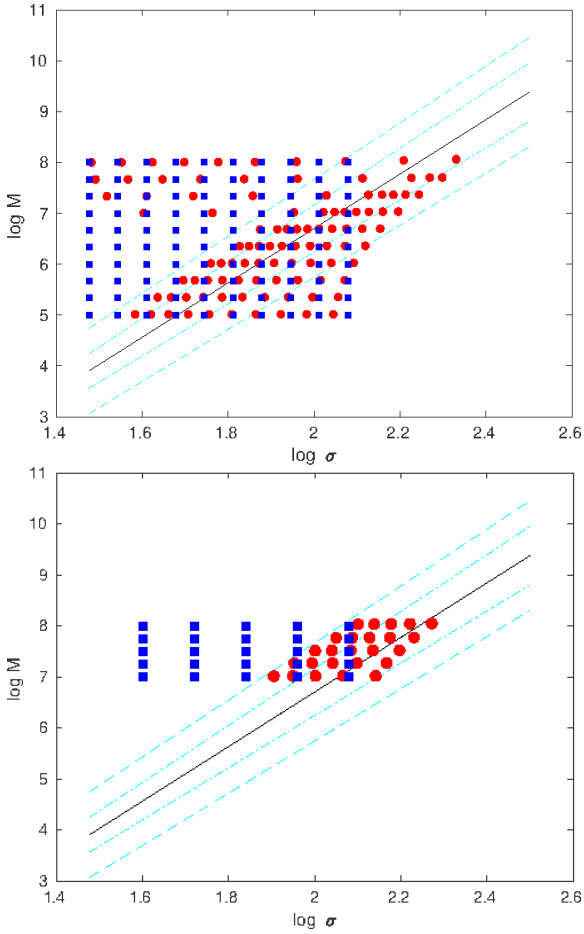


Figure 4. Upper plot: Log-uniform distribution of binary separations for 100 different initial conditions. Blue squares are the initial conditions. Red circles are the values after integration time of $t_{\text{final}} = 1.2 \times 10^{10}$ yr. The binary fraction we use is $f_{\text{binary}} = 1/2$, $a_{\text{min}} = 0.01\text{AU}$, $a_{\text{max}} = 100\text{AU}$ and $\alpha = 50$. The black solid line is the observed $M_{\bullet} - \sigma$ relation taken from [van den Bosch \(2016\)](#) and the 4 cyan lines indicates sigma uncertainty in slope and intercept. Lower plot: same as left plot with $t_{\text{final}} = 10^{12}$ yr.

the right plot of figure 4 the results of 25 integration with $t_{\text{final}} = 10^{12}$ yr.

Next we assume that the binaries sma have a log-normal distribution with mean value of $a_{\text{mean}} = 60\text{AU}$ ([Duchêne & Kraus 2013](#)). The lower bound of the sma is $a_{\text{min}} = 0.01\text{AU}$ and the upper bound is $a_{\text{max}} = 100\text{AU}$. The initial conditions are chosen to be identical as the previous case. The results are presented in figure 5. Similar to the log uniform case, the evolution of the initial condition mimics the observed $M_{\bullet} - \sigma$ relation for the mass range $5 < \log M_{\bullet} < 7$ for all calculated velocity dispersions, while for the initially more massive SMBH only velocity dispersion greater than $\sigma_0 \gtrsim 40\text{kms}^{-1}$.

Next we checked the stability of the $M_{\bullet} - \sigma$ relation. We set the initial conditions to be exactly on the observed relation and checked whether the binary disruption process destroys the $M_{\bullet} - \sigma$ relation. Figure 6 shows the results for both sma distributions.

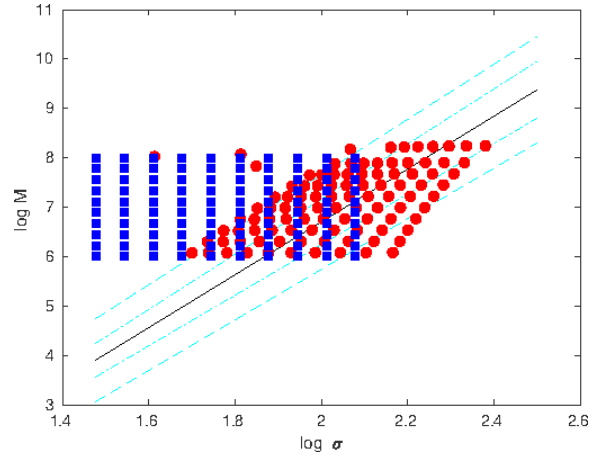


Figure 5. Log-normal distribution of binary separations. 100 different initial conditions. Here $a_{\text{mean}} = 60\text{AU}$. Blue squares are the initial conditions. Red circles are the values after integration time of $t_{\text{final}} = 1.2 \times 10^{10}$ yr. The binary fraction we use is $f_{\text{binary}} = 1/2$, $a_{\text{min}} = 0.01\text{AU}$, $a_{\text{max}} = 100\text{AU}$ and $\alpha = 50$. The black solid line is the observed $M_{\bullet} - \sigma$ relation taken from [van den Bosch \(2016\)](#) and the cyan lines are in figure 4.

4 DISCUSSION AND SUMMARY

Relaxation time and radial orbits

Our model is based on the assumption that the binary component which returns to the bulge immediately equilibrates its excess energy with its environment. In what follows we justify this assumption for lower end of the SMBH masses. The star that returns to the bulge interacts with its environment primarily via two-body interactions. Therefore the equilibrium timescale is the two-body relaxation timescale which is given by:

$$t_{\text{relax}} \approx \frac{\sigma^3}{8\pi G^2 m^2 n \ln \Lambda} \quad (24)$$

where m is the mean mass of the components, n is the number density and the Coulomb logarithm, $\ln \Lambda$, is defined as the natural log of the ratio between the two relevant length scales of the problem, the size of the environment, R , and the mean distance between the stars, $\sim n^{-1/3}$. The spatial region we focus on, i.e. the intermediate region (PM1), has a radius of $R \approx \alpha/2 \times r_h$ and a mass of $\sim \alpha \times M_{\bullet}$. Hence, for a $M_{\bullet} = 10^6 M_{\odot}$, $\alpha = 50$, and $\sigma = 50\text{kms}^{-1}$ the relaxation time is

$$t_{\text{relax}} \approx \frac{\alpha^2 G M_{\bullet}^2}{48 \sigma^3 \bar{m} \ln \Lambda} \approx 3 \times 10^9 \text{ yr} \left(\frac{M_{\bullet}}{10^5 M_{\odot}} \right)^2 \left(\frac{\sigma}{50 \text{ kms}^{-1}} \right)^{-3} \quad (25)$$

which is shorter than the Hubble time. However, the relaxation time for more massive SMBH are longer than Hubble time, therefore some stars may not equilibrate their excess energy with the bulge. These stars have higher speeds and move on an almost radial trajectories.

Binary disruptions that occur sufficiently late have no time to equilibrate their excess energy with the environment. Therefore, the surviving star will retain its velocity and have a radial trajectory within the bulge. As a result it will have distinctively different velocity than its neighboring stars. Can this be tested observationally?

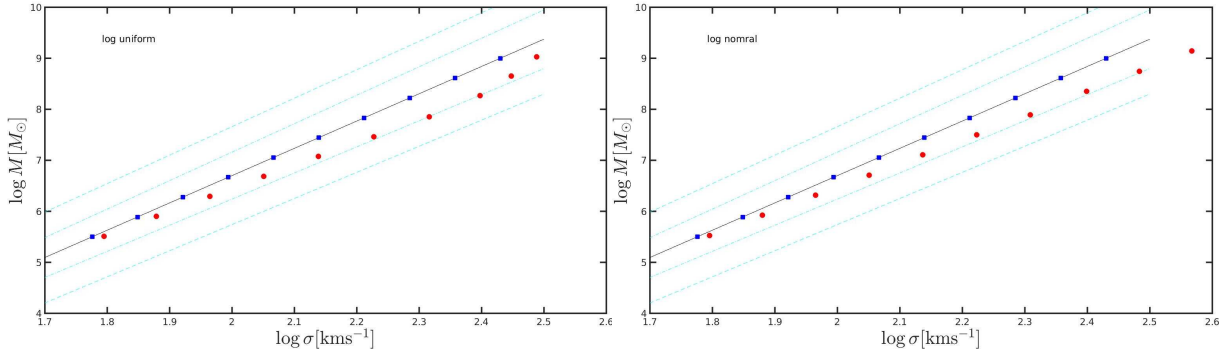


Figure 6. Left panel: For log-uniform sma distribution. Blue squares are the initial conditions on the best fit observed $M_{\bullet} - \sigma$ relation. The galaxy properties are the same as in figure 4. Red circles are the values after $t_{\text{final}} = 1.2 \times 10^{10}$ yr. Right panel: For log-normal case, galaxy properties the same as in figure 5.

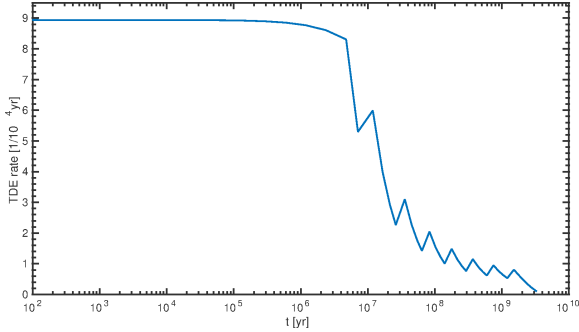


Figure 7. $\alpha = 50$, $M_{\bullet} = 1 \times 10^7 M_{\odot}$, $\sigma = 70 \text{ km s}^{-1}$, $a_{\text{min}} = 0.01 \text{ AU}$, $a_{\text{max}} = 100 \text{ AU}$, log-uniform distribution of the sma, $f_{\text{TDE}} = 0.1 \times \left(\frac{a}{\text{AU}}\right)^{-0.2244}$, and binary fraction of unity, $f_{\text{binary}} = 1$. TDEs rates are roughly constant for the first 10 Myr and decrease for the next $\sim 1 \text{ Gyr}$, as the binary population dwindles.

This might be a challenge for observers when attempting to determine the velocity dispersion from the width of some spectral lines. The current procedure assumes a homogeneous ensemble of stars, in contrast of what we predict here. A detail treatment of their implications on observational signatures will be the object of future work.

TDE rates

The proposed process produces a novel channel for TDEs, namely TDEs from binaries that originate from outside the sphere of influence. In figure 7 we present the TDE events per 10^4 years for a typical galaxy parameters, see caption. However, in figure 7 we assume a single star burst of single mass components, $m_{*} = 1 M_{\odot}$. We assume all stars are in their main-sequence stage of stellar evolution, hence have the same stellar radius, R_{*} . In order to study the implications of the proposed mechanism on the TDE rates the assumptions need to be relaxed. Therefore, we reserve a detailed analysis for the implications of TDEs rates and masses and stellar evolution for a future work.

Summary

We describe a novel explanation for the $M_{\bullet} - \sigma$ relation. In a triaxial potential, the intermediate spatial region, from

the radius of influence, r_h , up to $\sim 50 \times r_h$, from galactic centers, hosts chaotic trajectories of binaries. These binaries wander sufficiently close to the center of the potential in order for the binary to be tidally disrupted. As a result, one component loses energy and is usually captured by the SMBH or disrupted by it, while the other component gains energy and returns to the surrounding spheroid with excess energy. The excess energy may be equilibrated with the environment within a two-body relaxation time scale and hence changes the velocity dispersion. Essentially the SMBH splits the binaries and frees latent orbital energy and changes the kinetic temperature of the surrounding spheroid. The change in the kinetic temperature is equivalent to a change in the velocity dispersion that converges to the observed $M_{\bullet} - \sigma$ relation.

Our results are robust for SMBH masses $M_{\bullet} < 10^7 M_{\odot}$, namely galaxies with bulge masses lower than $10^7 M_{\odot}$ converge to the $M_{\bullet} - \sigma$ relation sufficiently fast. Accounting for galaxy evolution theory that suggests massive galaxies are build from the mergers of lower mass galaxies. The proposed mechanism described here indicates that lower mass galaxies are merging already close to their $M_{\bullet} - \sigma$ relation values and hence creates the merged, more massive galaxy, closer to its $M_{\bullet} - \sigma$ value.

ACKNOWLEDGEMENTS

EM thanks Richard Mushotzky and Coleman Miller for helpful and enlightening discussions.

REFERENCES

- Agnor C. B., Hamilton D. P., 2006, *Nature*, **441**, 192
 Anglés-Alcázar D., Özel F., Davé R., 2013, *ApJ*, **770**, 5
 Anglés-Alcázar D., Özel F., Davé R., Katz N., Kollmeier J. A., Oppenheimer B. D., 2015, *ApJ*, **800**, 127
 Bahcall J. N., Hut P., Tremaine S., 1985, *ApJ*, **290**, 15
 Duchêne G., Kraus A., 2013, *ARA&A*, **51**, 269
 Ferrarese L., Merritt D., 2000, *ApJ*, **539**, L9
 Gebhardt K., et al., 2000, *ApJ*, **543**, L5
 Gültekin K., et al., 2009, *ApJ*, **698**, 198
 Haan S., Schinnerer E., Emsellem E., García-Burillo S., Combes F., Mundell C. G., Rix H.-W., 2009, *ApJ*, **692**, 1623
 Hut P., 1981, *A&A*, **99**, 126

- Jahnke K., Macciò A. V., 2011, [ApJ](#), 734, 92
McConnell N. J., Ma C.-P., 2013, [ApJ](#), 764, 184
Merritt D., Poon M. Y., 2004, [ApJ](#), 606, 788
Peng C. Y., 2007, [ApJ](#), 671, 1098
Poon M. Y., Merritt D., 2001, [ApJ](#), 549, 192
Poon M. Y., Merritt D., 2002, [ApJ](#), 568, L89
Poon M. Y., Merritt D., 2004, [ApJ](#), 606, 774
Shen Y., et al., 2015, [ApJ](#), 805, 96
Stone N. C., Kesden M., Cheng R. M., van Velzen S., 2019,
[General Relativity and Gravitation](#), 51, 30
Zubovas K., King A. R., 2019,
[General Relativity and Gravitation](#), 51, 65
van den Bosch R. C. E., 2016, [ApJ](#), 831, 134